

Flow Behavior of Symmetrical P(S-*b*-MMA) Block Copolymers: Rheological Problems Arising from Shear Modified Morphology

H. BRAUN,* W. GLEINSER, and H.-J. CANTOW

Freiburger Materialforschungszentrum F.M.F., Albert-Ludwigs-Universität,
Stefan-Meier-Straße 31a, D-7800 Freiburg/i.Br., Germany

SYNOPSIS

In this article, symmetrical, narrow distribution P(S-*b*-MMA) block copolymers are characterized rheologically, using a dynamic spectrometer and a stress rheometer. The shear induced morphology changes are investigated by off-line electron microscopy and SAXS. We tried to correlate the results of dynamics and long-time creep experiments with morphological and rheological features. Summarizing, one can point out that the examined block copolymers reveal the well-known low frequency behavior of phase separated blends. Additionally, we observed a significant shear influence on the morphology, i.e. a shear induced structuring and alignment of lamellae. This considerable change in morphology is also reflected by characteristic rheological properties (retardation time, yield stress). Therefore, problems concerning the validity range of linear viscoelastic behavior arise, which are discussed in brief. © 1993 John Wiley & Sons, Inc.

INTRODUCTION

Recent developments in the polymer industry lead to more and more concern about polymer blends, block copolymers, composites, filled polymers, LC-polymers, or, generally speaking, about polymeric materials possessing more complicated structures as compared to homopolymers. Most of these materials show unusual rheological behavior (long relaxation times, yield behavior, significant strain dependence) and, therefore, even traditional rheometrical techniques are of doubtful value (e.g., concerning the initial equilibrium state) and should be improved or supplemented by other investigations. Therefore, it is important to perform morphology studies in addition to rheometry.

This article focusses on the rheological behavior of block copolymers. They are mainly used as compatibilizers in incompatible blends,^{1,2} toughening agents in brittle polymers, or, due to their regular equilibrium morphologies, as polymers with special

properties (e.g., triblock copolymers as thermoplastic elastomers,^{3,4} bicontinuous, anisotropic materials⁵). Numerous articles deal with S-B-S or S-I-S triblock copolymers,^{3,4} but little is known about pure thermoplastic diblock copolymer systems.⁶ In spite of several works concerning the rheology of block copolymers, as well as the dynamics of morphology changes during shear experiments, some questions remain open (at least in part):

- Does a suitable (structural) reference state exist and how should it be reached?
- What are the measuring conditions in order to ensure linear viscoelastic behavior, if shear induced morphology changes occur, especially in creep tests?
- In which way do morphology changes occur in lamellar diblock copolymers?
- Is the yield behavior influenced by shear induced morphology changes?

This article describes the comprehensive rheological and morphological characterization of three narrow distribution symmetrical P(S-*b*-MMA) block copolymers. The main task of the work does not consist

* To whom correspondence should be addressed.

in a presentation of numerous experimental data, but rather in an explanation of some significant results, as well as in the discussion of problems arising from rheometry and a rheological interpretation.

In the first section of the article, the materials used, the rheometrical devices (dynamical spectrometer, stress rheometer) and the techniques for investigation of the morphology [electron microscopy and small angle X-ray scattering (SAXS)] are described in detail. The experimental results are given in the second section. An extensive discussion, including a comparison with literature data, follows in the third section. We tried to correlate the results of dynamic and creep experiments, to compare block copolymers with corresponding blends, to give a physical explanation of the unusual flow mechanism observed, and to correlate the shear modified morphology with characteristic rheological quantities, such as yield stress and retardation time. Additionally, theoretical descriptions are briefly reviewed.

EXPERIMENTAL

Materials

Three symmetrical P(*S-b*-MMA) block copolymers were investigated. In order to obtain narrow distribution samples, they were synthesized by anionic polymerization at -85°C in THF with sec-butyl lithium as an initiator.⁷ The materials were purified by precipitation of a solution in THF (10 wt %) with methanol and were dried at 60°C under vacuum for at least two days. In order to suppress the thermal decomposition of PMMA, 2,6-di-*t*-butyl-4-methylphenol (0.1 wt %) was added.

DSC measurements on the block copolymers indicate two glass transition temperatures related to the components: $T_g(\text{PS}) = 102^{\circ}\text{C}$ and $T_g(\text{PMMA}) \approx 130^{\circ}\text{C}$. The elevated T_g of the PMMA component is caused by its special tacticity (80% syndiotactic and 20% heterotactic triads), resulting from the special polymerization conditions. The tacticity and the content of PMMA in the block copolymer was determined by $^1\text{H-NMR}$ spectroscopy. A summary of the block copolymers' characteristics is given in Table I.

For rheometry, sample discs were pressure-molded under vacuum at 180°C and were then dried, as described above. Gel permeation chromatography (GPC), before and after the rheological measurements, did not indicate any changes in molecular weight distribution, hence decomposition can be excluded under the conditions applied.

The upper critical solution temperature system,

Table I Characteristic Data of Block Copolymers ($U = M_w/M_n$)

	SM8	SM43	SM78
$M_n^{\text{PS a}}$ (g/mol)	7600	43,000	78,000
$U^{\text{PS a}}$	1.05	1.09	1.09
$M_n^{\text{ges a}}$ (g/mol)	13,000	73,000	126,000
$U^{\text{ges a}}$	1.18	1.12	1.17
wt % MMA ^b	53.5%	52.2%	52.8%

^a GPC: CHCl_3 , PS standard.

^b $^1\text{H-NMR}$: CDCl_3 , 80 MHz.

PS-PMMA, has an interaction parameter of $\chi = 0.028$.⁸ Taking into account the symmetry of the block copolymer, as well as the relation $(\chi N)_{\text{sep}} \geq 10.5$ (N is the degree of block copolymer polymerization, system P(*S-b*-MMA): $N_{\text{sep}} \approx 375$) for the microphase separation transition (MST), from Leibler's theory,⁹ one expects that SM43 and SM78 should be phase separated with a lamellar morphology. On the other hand, SM8 is not supposed to separate in the temperature range between glass transition and the decomposition, which is supported by our additional temperature-dependent SAXS measurements, showing a hypothetical MST temperature of -53°C for SM8.

Rheometry

Dynamical Spectroscopy

The dynamical measurements were carried out on a Rheometrics Mechanical Spectrometer (RMS-800) at temperatures between 150 and 230°C . For temperatures above 170°C , an inert N_2 atmosphere was used. Disc-and-plate fixtures (radius 12.5 mm) were adjusted with a gap of about 1 ± 0.2 mm, which varied from sample to sample. Due to the expected violation of the time-temperature superposition principle, the frequency range was extended as much as possible ($\omega = 100\text{--}0.001$ rad/s). The strain was varied between $\gamma = 1 \dots 30\%$ in order to obtain a measureable signal with respect to the transducer. It was difficult to determine the range of linear viscoelasticity, because no characteristic critical strain γ_{crit} exists, as known from homopolymers. Instead, a weak strain dependence is observed, even at low strains. It is much more pronounced for low frequencies and high measuring temperatures.

Stress Rheometry

The Rheometrics Stress Rheometer (RSR) was used to obtain the creep function (input: constant stress)

and yield stress (input: stress ramp) data. Shear induced morphology changes were expected, but the results obtained from experiments using 25-mm-diameter cone-and-plate (homogenous shear rate $\dot{\gamma}$), as well as disk-and-plate fixtures [$\dot{\gamma} = f(r)$], were nearly identical. Therefore, the latter was used for most of the measurements. All of the creep experiments explained below were carried out under an N₂ atmosphere at 200°C.

Some attention was paid to the drift behavior with respect to the measured quantities, because we intended to perform long-time creep and creep recovery investigations. The drift was relatively small, as compared to the absolute values (for creep < 1%, for recovery < 10%). Another problem arose concerning the desired long-time experiments: The RSR limits the maximum creep and recovery times each to about 36.4 h. This fact, as well as the transducers lower torque limit (required signal-to-noise ratio), made it impossible to decrease the shear rate in order to detect the terminal flow range. Nevertheless, the feasible one-and-a-half day experiments enabled us to extend the observation window up to one decade below the dynamical spectrometer's limits (up to $\dot{\gamma} \approx 10^{-5} \text{ s}^{-1}$).

Samples for morphology analysis (electron microscopy) were quenched below glass transition temperature for about 3 min controlling constant normal force and retaining the applied shear stress. This ensures a minimum destruction of the shear-induced morphology during quenching.

Electron Microscopy

Ultrathin cuts in two normal directions (radial and azimuthal) were always prepared from the sample bulk using a Leica Ultracut-E microtome with a diamond knife. The thickness of the specimens, indicated by their interference color, was about 60–70 nm. In order to improve contrast, the ultrathin sections were treated with RuO₄ vapor.

Transmission electron microscopy (TEM) measurements were carried out with a Zeiss CEM 902, operated with 80 kV. An 90 mm objective diaphragm was used, corresponding to an 17.3 mrad aperture in the back focal plane. All images were obtained from loss energy electrons.

Small Angle X-ray Scattering (SAXS)

A Kiesig camera was used in order to determine the lamellar dimensions, as well as the degree of orientation. Analyzing the SAXS patterns with Bragg's eq. (1), one obtains the lamellar periodicity (i.e.,

the distance between the centers of neighboring layers of the same polymer) of the nearly symmetrical block copolymer. The lamellar periodicity roughly equalled the thickness of both the PS and PMMA layer together.

$$n\lambda = 2d \sin \theta \quad (1)$$

Here, n is the reflection order, λ is the CuK_α wave length (0.154 nm), and θ is the scattering angle.

The degree of orientation can be determined from the azimuthal intensity distribution of the SAXS pattern. Unfortunately, the quality of our scattering patterns was insufficient for quantitative analysis, but sufficient to qualitatively reflect the orientation.

EXPERIMENTAL RESULTS

Mechanical Spectroscopy

The dynamic measurements are summarized in three master curves for the moduli (Figs. 1–3), at a reference temperature of about 180°C. The exact values and the appropriate shift factors a_T are listed in Figures 1–3. The three materials yield different behaviors with different aspects.

The SM8 sample behaves as a homopolymer below its entanglement molecular weight. This means that it is characterized by terminal flow, with a low frequency dependence of $G' \propto \omega^2$ and $G'' \propto \omega^1$, as well as a Rouse behavior at high frequencies ($G' \propto \omega^{0.5}$). This is not surprising, because the so-called Leibler rule (see *Materials*) only predicts long range structuring (forming lamellae) for a molecular weight higher than about 37,500 g/mol.

SM43 (Fig. 2) and SM78 (Fig. 3) reveal different behavior, because of their tendency to form a lamellar morphology. In spite of an extended measuring range (up to 10⁻³ rad/s), no terminal flow region occurs, and a terminal relaxation time could not be determined (even for the highest temperature). Instead, one observes the well-known dependencies, $G' \propto \omega^{0.5}$ and $G'' \propto \omega^{0.5}$ ($G' \approx G''$) at low frequencies, which are typical for phase separated block copolymers.^{10,11}

On the other hand, the high frequency behavior seems to be nearly unaffected by the lamellar structure. In order to analyze the entanglement behavior in the lamellar structured block copolymer melt, we tried to apply the Marvin-Oser equation,¹² which was primarily derived for homopolymers:

$$(\tan \delta)_{\min} = 1.04 \left(\frac{M_n}{M_c} \right)^{-0.8} \quad (2)$$

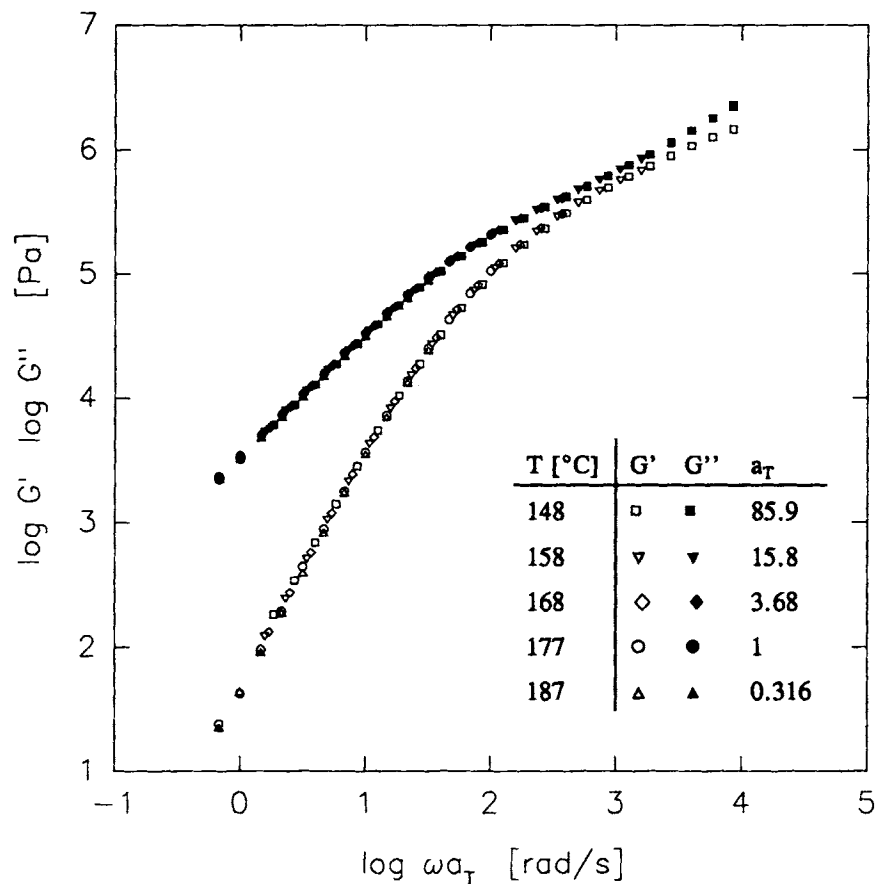


Figure 1 Master curves of the dynamic moduli G' and G'' ($T_{ref} = 177^\circ\text{C}$) for P(S-b-MMA) sample SM8.

Taking into account the critical molecular weights of the components (PMMA: $M_c \approx 3 \times 10^4$ g/mol, PS: $M_c \approx 3.3 \times 10^4$ g/mol), one obtains the M_n values of the appropriate single blocks only, but not of the whole block copolymer molecule. This means that the single blocks are responsible for the entanglement plateau measured. This seems reasonable, in view of the incompatibility of the different blocks, as well as the lamellar morphology.

Sample SM43 displays some peculiarities as compared to SM78. In contrast to the former, the individual frequency sweeps of SM78 can be shifted, that is, the time-temperature-superposition (TTS) principle holds true (at least approximately). Therefore, it is concluded that, in spite of an existing phase separated structure, no significant shear-induced morphology changes occur. On the other hand, the failure of the TTS principle for SM43 indicates a shear influence. The dynamic data cannot be shifted throughout the whole frequency range. For that reason, only the high frequency range, which was assumed to be nearly unaffected by morphology

changes, was used as a reference to derive master curves (Fig. 2). The low frequency part of these curves is successively lowered for increasing temperature. In this way, the little shoulder disappears and the final dependencies of G' and $G'' \propto \omega^{0.5}$ are approached step by step. The observed shear effect is more pronounced for G' than for G'' , which confirms the known fact that the storage modulus is more sensitive to morphology changes.¹⁰

Strain and time sweep experiments, on our SM43 sample, confirm that the shear-induced morphology changes reach a saturation level and that they are most significant at the highest measuring temperature (230°C) and the lowest frequencies. In contrast to other materials (e.g., SIS-block copolymers³), the shear structuring of the SM43 sample does not lead to a terminal flow range and, secondly, it seems that it achieves sufficient mobility for structuring only at extreme measuring conditions.

Summarizing the results obtained from dynamic spectroscopy, the SM43 sample seems to be suitable

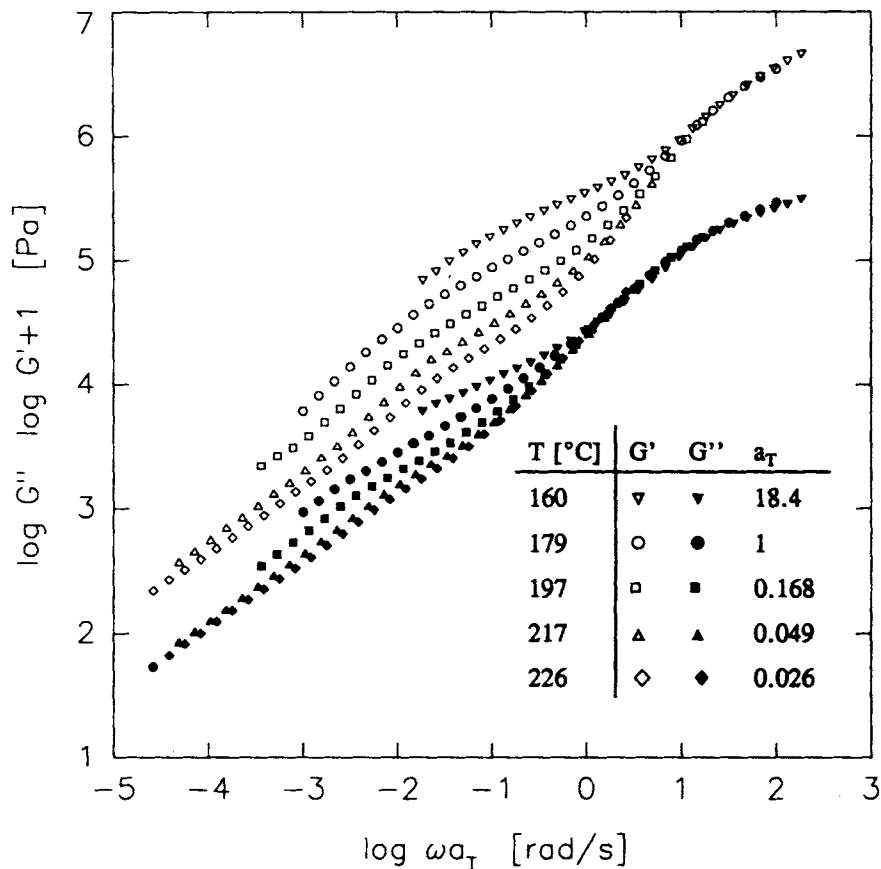


Figure 2 Master curves of the dynamic moduli G' and G'' ($T_{ref} = 179^\circ\text{C}$) for P(S-*b*-MMA) sample SM43.

to investigate morphology changes in further detail. In oscillatory shear flow, it behaves like a yield stress fluid and shows significant shear influence. Consequently, stress rheometry and electron microscopy studies have been performed.

Stress Rheometry

Is it possible to draw conclusions from stress rheometry concerning shear-induced morphology changes? We tried to analyze characteristic times (creep and recovery experiments), as well as yield stresses (stress ramp experiments). We selected some typical examples for this article.

First, we carried out a set of successive creep and recovery measurements, using the same sample. An applied stress of 50 Pa and a temperature of 200°C were chosen (see *Rheometry*, above). Figure 4 shows the first set of measurements, including four experiments. In this experiment, the creep time was varied from 10^2 to 10^3 , 10^4 , and 10^5 seconds. The recovery time was extended up to about one and a half days in some cases. The separate plots of the recoverable

strain [normalized to the measured or extrapolated maximum recoverable strain $\gamma_R = \gamma_{rec}(t \rightarrow \infty)$], dependent on time, are shown in Figure 5.

What are the characteristic features of the first set of creep and recovery experiments?

The reproducibility of the curves is relatively poor, as compared to investigations of homopolymers, for example. We assume that the undefined initial morphology may be responsible for this. However, the creep curve can be divided into two power-law sections, with slopes to the logarithmic plot (Fig. 4) of about 0.58 and 1, respectively. The logarithmic slope of 1 indicates that the block copolymer sample behaves like a fluid at strains larger than about 5–8 units, corresponding to a creep time of about 5×10^4 s. A quantitative comparison between the creep flow (RSR) and the low frequency dynamic (RMS) experiments also confirms the Cox-Merz rule [$\eta(\dot{\gamma}) \approx \eta^*(\omega = \dot{\gamma})$] within the limits of experimental error.

The recovery also shows some interesting features. Nearly the whole creep deformation (up to $\gamma = 0.2$) recovers, if the creep time does not exceed

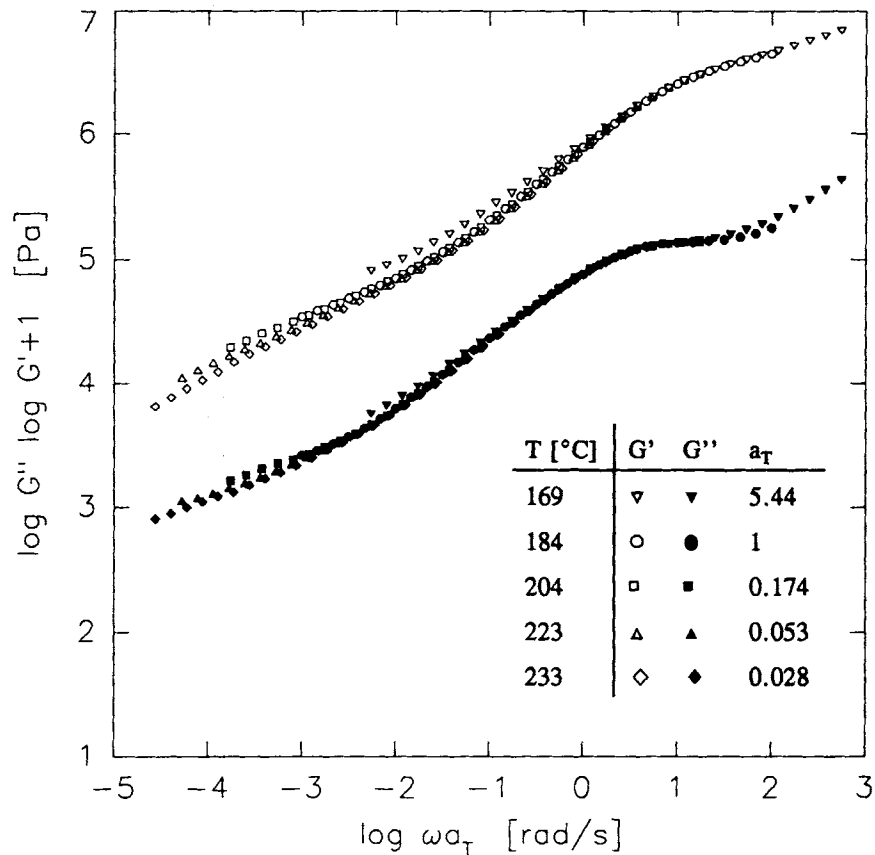


Figure 3 Master curves of the dynamic moduli G' and G'' ($T_{ref} = 184^\circ\text{C}$) for P(S-b-MMA) sample SM78.

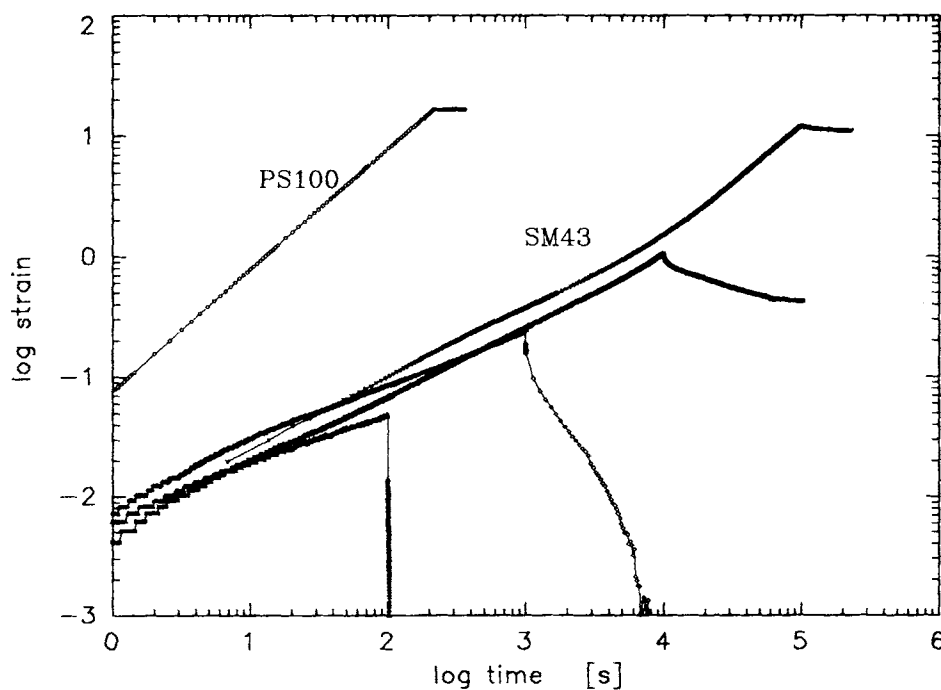


Figure 4 First set of creep and recovery experiments for P(S-b-MMA) sample SM43 at $T = 200^\circ\text{C}$, creep times: 10^2 , 10^3 , 10^4 , and 10^5 s; PS ($M_w = 10^5$ g/mol) for comparison.

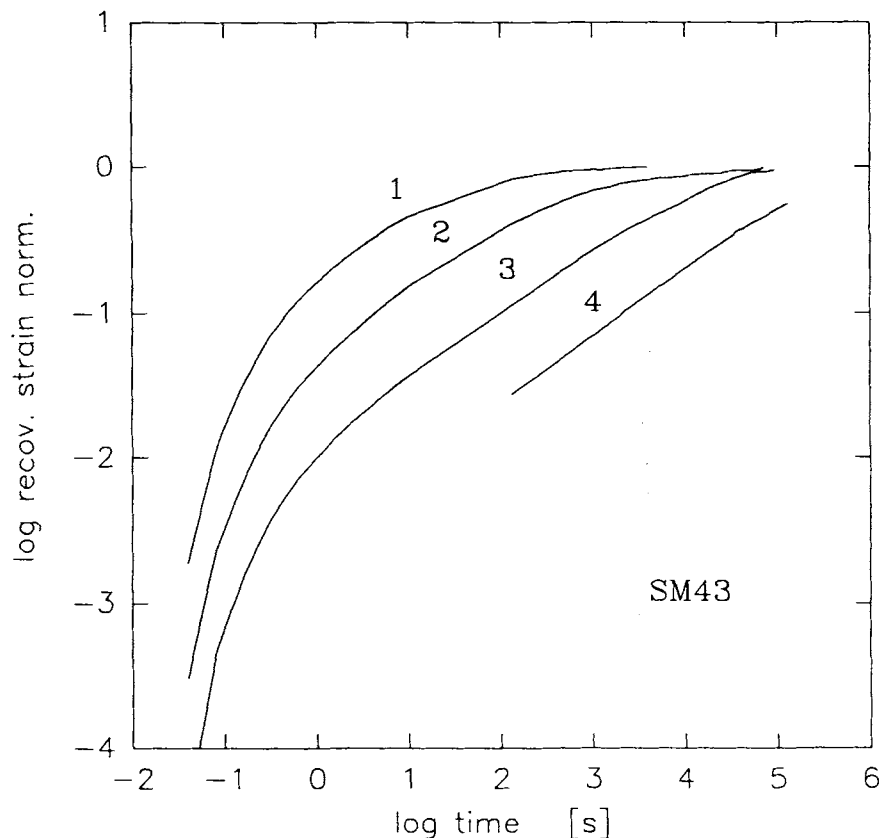


Figure 5 Normalized recoverable strain curves [reference $\gamma_{\text{rec}}(t \rightarrow \infty)$] of P(S-*b*-MMA) sample SM43 from the first set of creep experiments (creep times before recovery: 1 \rightarrow 10^2 s, 2 \rightarrow 10^3 s, 3 \rightarrow 10^4 s, and 4 \rightarrow 10^5 s; $T = 200^\circ\text{C}$).

10^3 seconds. However, it is not an instantaneous, but rather a delayed, recovery. Further increasing of the creep time also increases the recoverable strain up to about $\gamma_R \approx 2$ (compared with an appropriate PS ($M_w \approx 10^5$) $\gamma_R \approx 0.03^{13}$), but an irreversible deformation remains. A more significant power-law behavior is also observed for the recovery zone (Fig. 5) with a slope of about 0.46 in the logarithmic plot. Flow behavior, characterized by such a power-law slope, has been already discussed in literature,²⁶ albeit in another context. It is assumed that this is caused by cooperative phenomena. This also seems to apply to our lamellar-oriented block copolymers.

The recovery times, λ_i [which are the times after which the transient quantities (e.g., strain) achieve about 95% of the steady state value] increase with increasing creep time and reach a maximum value, if steady shear is achieved in the creep before recovery. A significant difference between characteristic times in creep and recovery is observed. Thus, the creep retardation time during creep ($\lambda_1 \approx 5 \times 10^4$ s, measured in the longest creep experiment), obtained from the purely elastic contribution (i.e.,

creep curve minus viscous flow), is much smaller than the corresponding extrapolated (!) recovery time ($\lambda_2 \approx 10^6$ s), indicating different structuring processes in the two phases of the experiment. This means that the destruction of an initial morphology (e.g., grains of the pressure-molded sample or the partly oriented domains after the first short creep experiments), and the shear structuring, occur much faster than the equilibration or the restructuring during the recovery.

After a sufficiently long annealing time, the four experiments described above are repeated in a second set. For clarity, only the two experiments with a creep time of 1000 s are presented in Figure 6. In principle, similar creep and recovery behavior was observed qualitatively. However, two remarkable points should be emphasized (cf. Fig. 6), which result from the flow history (first set of measurements):

- The fluidity of the sample is increased (power-law slope of the creep curve is now about 0.7–0.8 and the irreversible strain is increased).
- The characteristic recovery times are much

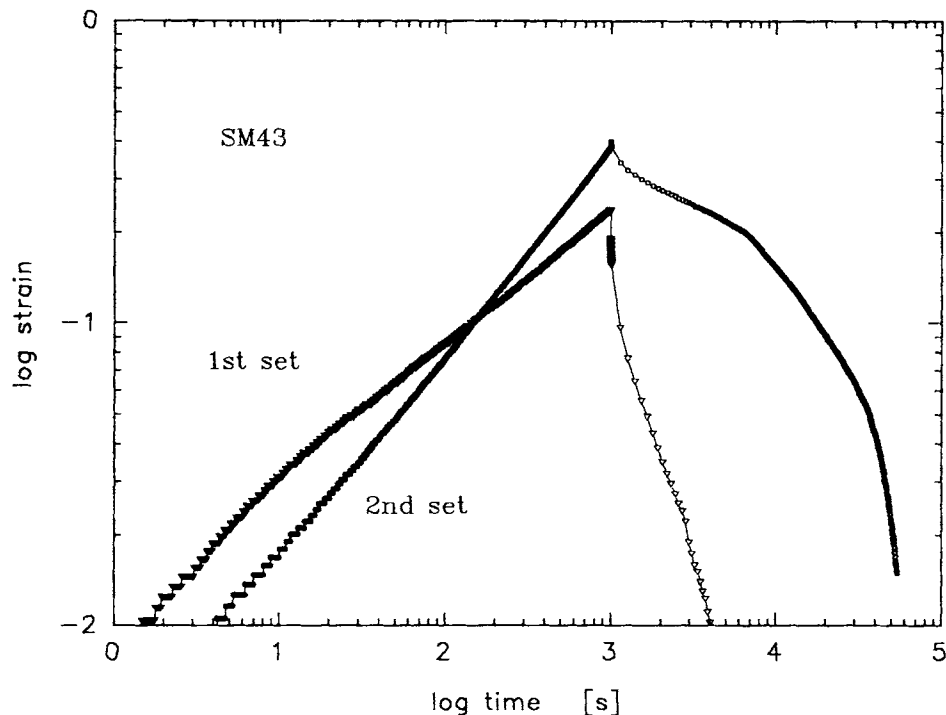


Figure 6 Comparison of two creep and recovery experiments (from the 1st and 2nd set of measurements) of P(S-*b*-MMA) sample SM43 with a creep time of 10^3 s at $T = 200^\circ\text{C}$.

longer than before (significant especially for experiments with the shorter creep times up to 10^3 s), that is, the recovery is delayed.

In spite of the unexpected fluidlike behavior, the results obtained by stress rheometry correlate well with the observations made in the dynamic experiments (RMS) at low frequencies (especially the decreasing elastic contributions, due to flow-induced morphology changes). This means that the supposed morphology changes are also reflected in creep and recovery experiments. However, the question remains open: which are the characteristic structuring processes responsible for the rheological behavior observed? To answer this question, three samples were prepared for electron microscopy; one after pressure molding and the others quenched during steady flow and after recovery (see below).

The stress rheometer (with stress ramp mode) was also used to determine yield stresses. Such measurements were always carried out between the creep experiments described above. Taking into account the final results from creep tests, that is, the fact that the block copolymer behaves like a fluid, one does not expect a classical yield stress. Is it possible to verify it and does a yield stress occur in the pressure-molded block copolymer before any viscous flow is induced?

Indeed, a yield stress τ_y of about 5–11 Pa is measured, if a stress ramp with $\dot{\tau} = 0.2 \text{ Pas}^{-1}$ is applied on an unsheared sample and τ_y vanishes after viscous shearing. In contrast to usual yield stress, a temperature dependence of τ_y was observed (τ_y decreases if T increases). Variations in the stress ramp conditions ($\dot{\tau} = 0.02, 0.2, 2 \text{ Pas}^{-1}$) reveal this interesting behavior: The faster the ramps are, the higher the τ_y values that are observed. Furthermore, the strain behavior for $\tau < \tau_y$ is surprising, but may be due to transducer drift¹⁴: A deformation occurs in the opposite direction and seems to be compensated for before the expected behavior is observed for $\tau > \tau_y$. This “negative overshoot” depends also on the ramp conditions (the overshoot is more pronounced for decreasing $\dot{\tau}$). Effects of a previous experiment (e.g., an uncompleted recovery) can be excluded, because this behavior is not observed in such experiments carried out after the first viscous flow of the sample. It is interesting to note that the surprising strain effects have never been observed with PS.

Summarizing the yield stress measurement results, some significant peculiarities were observed, which are difficult to explain, even by advanced theoretical descriptions, including so-called durability effects.¹⁵ Nevertheless, it seems that the pressure-molded sample has a morphology with yield stress properties and that a build-up of flow struc-

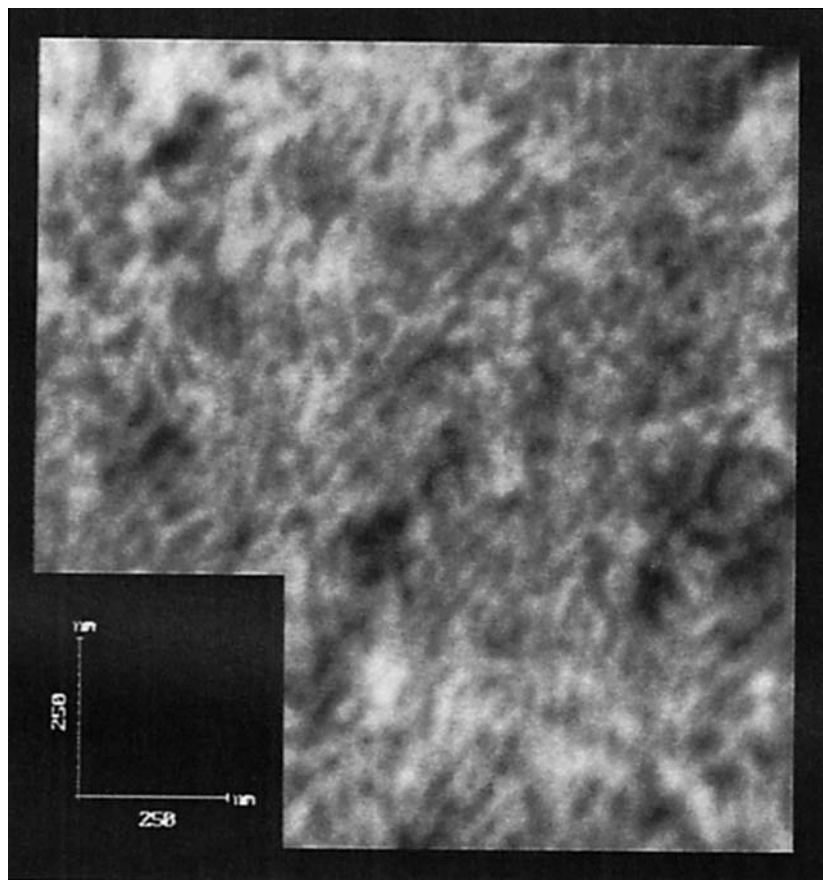


Figure 7 TEM image of an unsheared P(S-*b*-MMA) sample SM43.

tures (highly oriented lamellae) occurs during shear, resulting in a vanishing yield stress in subsequent creep experiments. Finally, the question concerning a stable reference state remains open. It should be emphasized that the yield stress behavior, described above, was observed in most, but not all of our experiments. In one case, the peculiar yield behavior remained also after viscous flow of the sample.

Electron Microscopy and SAXS

Some characteristic electron microscopy images are selected for the present article. They correspond to a pressure-molded, unsheared sample (Fig. 7), and to RSR samples, which were quenched during viscous flow (Fig. 8) and after recovery (Fig. 9). It should be mentioned that there was no significant difference between the radial and azimuthal cuts in all three cases. Therefore, no distinction in terms of cut orientation is made. For the unsheared, pressure-molded sample, we find an isotropic morphology with well dispersed block copolymer grains of about 0.1–0.2 μm in size. This is not surprising. However, the block copolymer should have a la-

mellar structure, corresponding to the thermodynamic equilibrium. Therefore, one expects that the equilibration may be facilitated by a shear-induced activation process. Indeed, one can see from Figure 8 that an enormous shear alignment, that is, a highly ordered lamellar structure, is obtained by creep. The characteristic lamellar periodicity distance was found to be about 33 nm. In contrast to the lamellar distance determined by electron microscopy, the SAXS measurements yield about 26 nm and a model prediction¹⁶ yields about 50 nm, according to eq. (3).

$$d = 0.024 M_n^{2/3} \quad (3)$$

Here, d is the periodicity of the lamellae and M_n is the number average molecular weight of the block copolymer. The deviation from the model prediction may be explained by the use of a different block copolymer composition (our block copolymer consists of two amorphous polymers, in contrast to block copolymers with one elastomeric component, as in Ref. 16). However, the large difference between electron microscopy and SAXS results is hard to understand.

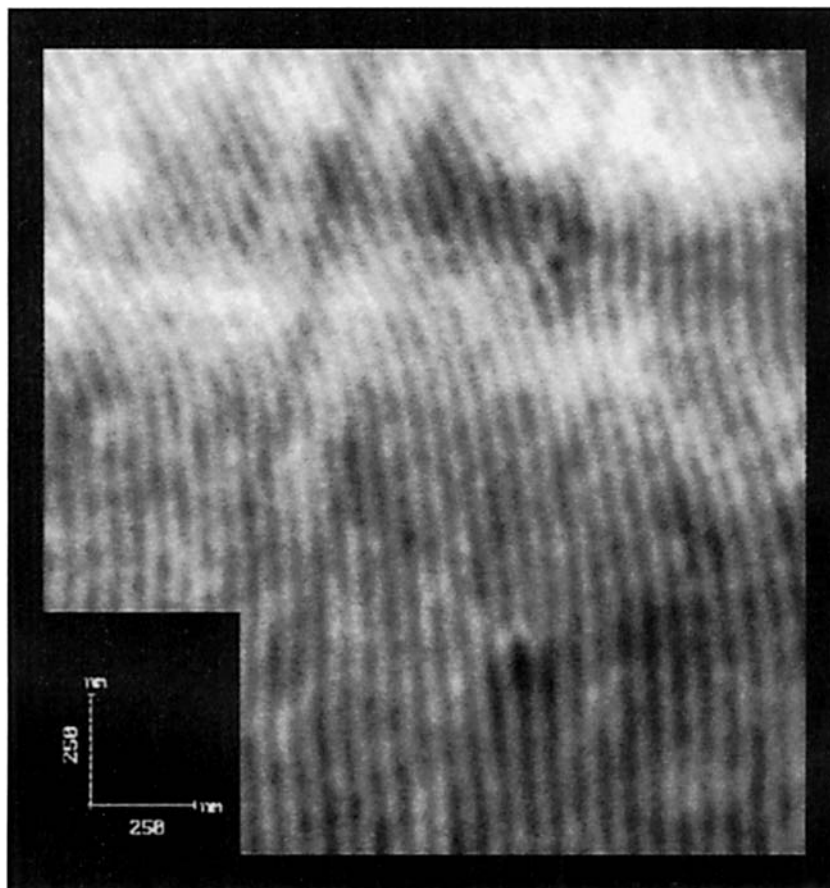


Figure 8 TEM image of P(S-*b*-MMA) sample SM43, quenched during steady creep after about 10 strain units, at $T = 200^{\circ}\text{C}$.

Figure 9 shows the morphology after recovery, where we find a so-called onion pattern. This is unexpected, with respect to the highly ordered lamellae under shear before, but it is confirmed by numerous images. On the other hand, it would explain the difference observed between the characteristic retardation times in creep and recovery, respectively. One can see that the equilibrium morphology under shear does not correspond to the one in recovery. Healing internal stresses, possibly caused by some defects, may be considered as a driving force.

DISCUSSION

Before we discuss the main features, which were observed on the block copolymers, they are listed in a brief summary once more. Our block copolymers show (i) a shear induced morphology change from a disordered nonequilibrium grain structure to an equilibrium lamellar structure, (ii) a deformation-dependent yield stress behavior, (iii) extremely long characteristic times, high viscosities, and large re-

coverable strains, as well as (iv) an asymmetry between recovery and the elastic part of creep. Finally, various problems concerning the validity range of linear viscoelasticity are obvious, which generally arise for complex polymeric materials.

Different mechanisms, responsible for the unusual rheological behavior of polymeric materials with a complicated structure, are known. With respect to the block copolymers considered, processes such as (i) constraint reptation of polymer chains with one end fixed, (ii) cooperative reptation, due to thermodynamical forced alignment of chains, and (iii) healing of structural (lamellar) defects, are important at low frequencies (or long measuring times), in addition to the well-known high frequency behavior. The following discussion is mainly restricted to the low frequency (long time) behavior.

The block copolymer in the form of the pressure-molded, unsheared sample, and in the partly oriented RMS sample, consists of nonequilibrated grains, which are linked to each other by flexible, reptational polymer chains. These entanglements

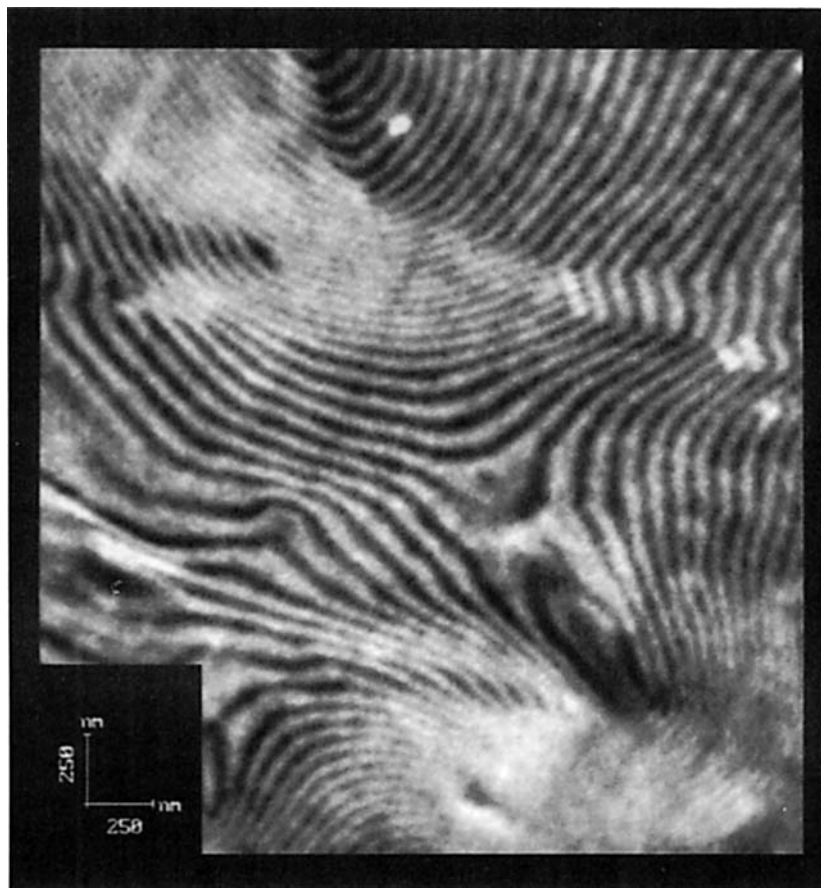


Figure 9 TEM image of P(S-*b*-MMA) sample SM43 two days recovered at $T = 200^\circ\text{C}$ after steady creep.

on the grain boundaries seem to be dominant as compared with the processes within the grains. This is reasonable, because of the large internal interface corresponding to the numerous small interacting grains.³ Therefore, a deformation and rate-dependent yield stress behavior may be explained in contrast to a constant yield value, known from suspensions of rigid particles.

Starting our creep experiment, the deformation energy density, $\tau\gamma_e$ (τ , creep stress imposed; γ_e elastic strain), increases with time to exceed a critical value and causes a modification of morphology (grain configuration). But in which way? Little is known about the structuring process, but some interesting facts are obtained from knowledge of the morphology under steady shear conditions, which follow.

According to eq. (4), the free enthalpy density of mixing ΔG_{mix} , which is responsible for a thermodynamical forced structuring (lamellar morphology), can be determined⁴ for our SM43 block copolymer:

$$\Delta G_{\text{mix}} = RT \left[\frac{\Phi_{\text{PS}} \ln \Phi_{\text{PS}}}{V_{\text{PS}} N_{\text{PS}}} + \frac{\Phi_{\text{PMMA}} \ln \Phi_{\text{PMMA}}}{V_{\text{PMMA}} N_{\text{PMMA}}} + \frac{\chi \Phi_{\text{PS}} \Phi_{\text{PMMA}}}{(V_{\text{PS}} V_{\text{PMMA}})^{1/2}} \right] \quad (4)$$

Here, R is the gas constant, T is the temperature, V_i is a molar volume ($V = M/\rho$, M : molecular weight, ρ : mass density), Φ_i is a volume fraction ($\Phi_i = V_i/(V_{\text{PS}} + V_{\text{PMMA}})$), N is the degree of polymerization and χ is the Flory-Huggins parameter. In this way, one obtains $\Delta G_{\text{mix}} \approx 125 \text{ Pa}$ for SM43 at 200°C . The flow energy density, in a creep experiment at 50 Pa, matches this value at about 2.5 (elastic) strain units, and will destroy the thermodynamically imposed structure. However, what we observe is a highly ordered lamellar morphology in steady flow. Therefore, one can conclude for steady flow both that the elastic stored energy density is lower than ΔG_{mix} and that the irreversible flow mechanism (i.e., the reptation process of entangled

blocks between the lamellae), observed at the chosen conditions, is characterized by the amount of actual stationary stored elastic energy. As mentioned above, the latter can be determined by subtracting the flow term from the creep curve. One obtains a characteristic energy density of about 18 Pa, which can be interpreted as a flow activation energy. However, it has another meaning than the Arrhenius activation energy for thermally stimulated processes ($E_a \approx 3.6 \times 10^6$ Pa calculated for SM43).

At first sight, the existence of a highly oriented lamellar morphology with expected flow in "homopolymer" layers does not seem to be consistent with the extreme long retardation times and the enormous elasticity. On the other hand, well defined flow zones, formed in the first set of creep experiments, would explain the vanishing yield stress behavior in the second set of measurements. In contrast to the nearly isotropic morphology of the pressure-molded sample, the lamellar structure is an anisotropic bicontinuous one. Therefore, we measure only the flow properties between the lamellae. Compared to homopolymers, cooperative phenomena of neighboring (block) chains, as well as constraint reptation processes of chains with one end fixed, become dominant. Indeed, these processes can be regarded as reasons for the high melt elasticity and the corresponding long retardation times. Doi and Kuzuu¹⁷ proposed a modified tube model for the reptation of polymer chains with a fixed end. Such reptation is strongly hindered and, following their theory, it requires an additional activation process, leading to a retarded motion. Star-branched polymers,¹⁸ micellar morphologies,¹⁹ as well as liquid crystal polymers,^{20,21} show similarities to the flow behavior of block copolymers. This is reasonable, because the shear influence on LC polymer domains with varying director orientations is comparable with the grain morphology of our pressure-molded sample and, on the other hand, the final lamellar flow layers in block copolymers may be approximated by interacting "micelles" of infinite diameter. As in the LC polymer system,²¹ the flow layers of our oriented block copolymer samples have a lower viscosity as compared to the polydomain or polygrain sample. However, the flow mechanism between lamellae is not the classical terminal flow, but rather a stable pseudo-flow process, characterized by well defined dependencies. Such systems have large values of relaxation times and an exponential enhancement, rather than a power-law dependence on the molecular weight, as known from the homopolymers.

Another theoretical approach, based on models with fractional derivatives,²² should be mentioned.

Without any direct relation to the molecular quantities, the description on an empirical level accounts for the power-law behavior observed over some decades in rheological measurements of the block copolymers.

Summarizing the elastic behavior, the following comparison of recoverable strains γ_R (or recoverable compliance J_{eo}) illustrates the enormous differences between homopolymers, blends and block copolymer:

PS : PMMA : PS-PMMA blend :

$$P(S-b-MMA) \approx 1 : 2 : 8 : 70$$

Here, the relation between the homopolymers and the blend was derived from Ref. 23, and the PS value ($M_w \approx 110,000$) from Ref. 13, whereas the block copolymer was measured by us.

Finally, the theory of linear viscoelasticity (e.g., Schwarzl²⁴) and its applicability in rheology is discussed. In contrast to homopolymers, the understanding of the assumptions and conditions of linear viscoelasticity is poor for complex materials. Therefore, some problems arise with respect to the validity range. In order to apply the relationships of the linear viscoelasticity theory, one has to ensure deformation conditions in the linear range of deformation. What does this mean for usual experiments? It was shown that, exceeding a critical strain in a kinematically controlled experiment, as well as a critical stress in a stress controlled experiment, leads to nonlinear effects. In other words, a creep experiment requires the following conditions in order to yield linear viscoelastic measurements: (i) a constant (Newtonian) viscosity, corresponding to an existence of a terminal flow zone, (ii) the onset of flow at a characteristic, stress independent time, (iii) a stable morphology, and (iv) an asymptotic growth of the normal force during creep without any overshoot. Investigating complex materials, one knows that most of these requirements are not fulfilled. Indeed, for materials with a second shear thinning range at low shear rates, with special scaling laws,²⁵ or with significant shear effects on structure, the application of the theory of linear viscoelasticity is not justified in transient or steady experiments such as creep.

Nevertheless, rheological data, obtained from complex materials, can be interpreted in some modified ways. The phenomenological Cox-Merz rule, for example, allows a correlation of linear dynamic data and nonlinear transient results within the lim-

its of experimental error [e.g., $\eta(\dot{\gamma}) \rightarrow \eta^*(\omega)$] and, thus, a common analysis in the framework of linear viscoelasticity is partly possible.

In spite of some restricted cases, where the linear theory is applicable, it will be more and more necessary to carry out and to analyze nonlinear experiments with nonlinear constitutive theories directly. In this way, it is easier to determine characteristic parameters, such as retardation times, yield stresses, and elastic contributions and to achieve adequate descriptions and modelling.

CONCLUSIONS

Generally, to obtain reliable rheological characteristics of block copolymers or similar complex materials was a difficult methodological problem. Due to an inevitable shear influence on morphology, the questions of the importance of linear viscoelastic measurements and an extended validity range should be analyzed once more in order to apply well-known theoretical descriptions. In contrast to a commonly accepted opinion, we recommend transient or steady rheological experiments, such as creep, stress growth, and stress relaxation. Such experiments yield valuable information (e.g., characteristic times, threshold values, and elastic contributions) in a more direct way and, sometimes, its interpretation is facilitated. Of course, the nonlinearity of these experiments requires an analysis using nonlinear theories.

Our experiments also revealed some inadequacies in the available rheometrical devices, which are developed essentially for homopolymers. Investigations of complex polymeric materials required extended measuring ranges (low frequencies, long times), an improved drift behavior, simultaneous morphology studies (e.g., light scattering methods), and implemented, advanced theoretical methods for analysis.

This work was supported by the Bundesministerium f. Forschung und Technologie, BMFT, and the BASF AG. We also acknowledge C. Auschra (University of Mainz) for preparing the samples, P. Zutavern for electron microscopy studies, and Dr. Chr. Friedrich for valuable discussions.

REFERENCES

1. C. Wippler, *Polym. Bull.*, **25**, 357 (1991).
2. W. H. Jo, H. C. Kim, and D. H. Baik, *Macromolecules*, **24**, 2231 (1991).
3. F. A. Morrison, G. Le Bourvellec, and H. H. Winter, *J. Appl. Polym. Sci.*, **33**, 1585 (1987).
4. F. A. Morrison, H. H. Winter, W. Gronski, and J. D. Barnes, *Macromolecules*, **23**, 4200 (1990).
5. J. Lehrke, K. Crämer, H. Lüchow, and W. Gronski, *Makromol. Chem. Rapid Commun.*, **11**, 495 (1990).
6. W. Gleinser, H. Braun, and Chr. Friedrich, *Mechanical Spectroscopy of P(S-*b*-MMA)-Copolymers*, IUPAC-Meeting, "Rheology of Polymer Melts," Prag, 1991.
7. R. D. Allen, S. D. Smith, T. E. Long, and J. E. McGrath, *Polym. Prepr.*, **27**, 54 (1986).
8. T. P. Russel, R. P. Hjelm, and P. A. Seeger, *Macromolecules*, **23**, 890 (1990).
9. L. Leibler, *Macromolecules*, **13**, 1602 (1980).
10. F. S. Bates, *Macromolecules*, **17**, 2607 (1984).
11. J. H. Rosedale, and F. S. Bates, *Macromolecules*, **23**, 2329 (1990).
12. H. Oser and R. S. Marvin, *J. Res. Nat. Bur. Stand.*, **67B**, 87 (1963).
13. G. Marin and W. W. Graessley, *Rheol. Acta*, **16**, 527 (1977).
14. A. Magnin and J. M. Piau, *J. Rheol.*, **35**, 1465 (1991).
15. A. Y. Malkin, *Rheology of Filled Polymers*, In: Advances in Polymer Science 96, Springer-Verlag, Berlin, Heidelberg, 1990.
16. G. Riess and G. Hurtrez, *Encycl. Polym. Sci. & Eng.* 2nd Ed., **2**, 324 (1985).
17. M. Doi and N. Kuzuu, *J. Polym. Sci. Polym. Lett. Ed.*, **18**, 775 (1980).
18. K. Osaki, E. Takatori, M. Kurata, H. Watanabe, H. Yoshida, and T. Kotaka, *Macromolecules*, **23**, 4392 (1990).
19. H. Watanabe and T. Kotaka, *Macromolecules*, **17**, 342 (1984).
20. T. Asada, H. Muramatsu, R. Watanabe, and S. Onogi, *Macromolecules*, **13**, 867 (1980).
21. R. G. Larson and D. W. Mead, *J. Rheol.*, **33**, 1251 (1989).
22. Chr. Friedrich and H. Braun, *Rheol. Acta*, **31**, 309 (1992).
23. B. A. Thornton and R. G. Villasenor, *J. Appl. Polym. Sci.*, **25**, 653 (1980).
24. F. R. Schwarzl, *Polymer Mechanik*, Springer-Verlag, Berlin, Heidelberg, 1990.
25. R. G. Larson and M. Doi, *J. Rheol.*, **35**, 539 (1991).
26. S. Matsuoka, *Relaxation Phenomena in Polymers*, Hanser, New York, 1992.

Received April 2, 1992

Accepted September 21, 1992